



A Mathematical Model for the Transmission Dynamics of COVID-19 Pandemic Considering Protected and Hospitalized with Optimal Control

Tinaw Tilahun Asmamaw¹, Kiros Gebrearegawi Kebedow^{2,*}

¹Department of Mathematics, Mezan Tepi University, Ethiopia

²Department of Mathematics, Hawassa University, Ethiopia

KEYWORDS

COVID-19;
Protection;
Stability analysis;
Forward
bifurcation;
Sensitivity
analysis;
Optimal control

ABSTRACT

In this paper, we propose a mathematical model to investigate coronavirus diseases (COVID-19) transmission in the presence of protected and hospitalized classes. We establish that the solution of the dynamical system remains positive and bounded. We compute the disease free equilibrium point and analyze the stability behavior of the steady state solutions. We determine the basic reproduction number (R_0) and demonstrate that the disease fades away when $R_0 < 1$ but persists in the population when $R_0 > 1$. The center manifold theory is used to assess the local stability of the endemic equilibrium. The model demonstrates a forward bifurcation, and a sensitivity analysis is conducted. The sensitivity analysis reveals that R_0 is highly influenced by the protection rate, highlighting the necessity of maintaining a high level of protection along with hospitalization to effectively control the disease. We develop optimal strategies for protection and hospitalization. The characterization of the optimal control is derived using Pontryagin's Maximum Principle. Numerical results for the dynamics of the COVID-19 outbreak and its optimal control show that a combination of protection and hospitalization is the most effective strategy for reducing the spread of COVID-19 within the population..

Research article

1. INTRODUCTION

Coronavirus disease 2019 (COVID-19) is an infectious disease caused by a newly discovered coronavirus [Gurmu et al. \(2020\)](#). The new virus was first appeared late December 2019 in the Chinese city of Wuhan and eventually invaded the world due to fast modern air trans-

portation [Lemecha Obsu and Feyissa Balcha \(2020\)](#). The novel coronavirus- now referred to as COVID-19 is caused by severe acute respiratory syndrome (SARS-CoV-2) and consists of single-stranded ribonucleic acid (RNA) structure [Sohrabi et al. \(2020\)](#).

The novel coronavirus is mainly spread

Corresponding author

Email address: kirosg@hu.edu.et +251926528484

<https://dx.doi.org/10.4314/eajbcs.v5i2.55>

from person to person, through respiratory droplets, the spread is more likely when people are within 6 feet of each other [Toquero \(2020\)](#). There is no known curing medicine to combat the COVID-19 pandemic. Standard recommendations by the WHO to prevent the spread of COVID-19 include frequent cleaning of hands using soap or alcohol-based sanitizer, covering the nose and mouth with a flexed elbow or disposable tissue when coughing and sneezing and avoiding close contact with anyone that has a fever and cough [Toquero \(2020\)](#).

Mathematical modeling in epidemiology helps to understand the fundamental mechanisms that drive the spread of disease, while also offering insights into potential control strategies. The model formulation process clarifies the assumptions, variables, and parameters involved. Furthermore, models offer conceptual insights such as thresholds, basic reproduction numbers, contact numbers, and replacement numbers. Mathematical models and computer simulations are useful experimental tools for building and testing theories, assessing quantitative conjectures, answering specific questions, determining sensitivities to changes in parameter values, and estimating parameters from data [Brauer et al. \(2019\)](#).

The first mathematical model was developed by Daniel Bernoulli [Allen et al. \(2008\)](#) on pandemic of smallpox by introducing two systems of ordinary differential equations. He assumed that recovery from infection confers immunity (no re-infection). He also assumed that the probability that infected individuals for the first time die does not depend on those who survive from the infection. He showed that inoculation was advantageous if the associated risk of dying was less than 11%.

A number of compartmental models have been proposed and analyzed for the COVID-19 outbreak in different countries. In particular, Yang and Wang [Yang and Wang \(2020\)](#) proposed a mathematical model for COVID-19 incorporating multiple transmission pathways, including both human-to-

human and environment-to-human transmission routes. Global stability was analysed using Lyapunov function. The authors employed a bilinear incidence rate based on the law of mass action and fitted the model with the data of Wuhan city of China and estimated the reproduction number.

In 2020, Haileyesus and Getachew [Alemneh and Telahun \(2020\)](#) proposed a conceptual SEIR model to study the pandemic COVID-19 transmission in Ethiopia. Global stability was analysed using Lyapunov function. Additionally, they incorporated time-dependent controls into the basic model and extended it to an optimal control framework for the disease. An optimal control problem was formulated and analyzed using Pontryagin's Maximum Principle. However, none of the authors cited here are considering protected and hospital-ized classes with optimal controls. Thus we are improved the existed model, by including the protected and hospitalized classes with optimal controls.

The remainder of the paper is organized as follows. In Section 2 we provided the description of the problems and its mathematical model formulation. Section 3 gives details the qualitative analysis of the model. The numerical analysis of our model is presented in Section 4, furthermore we present the extensions of the model to optimal controls and its numerical simulations 5 and 6. Finally, Section 7 concludes the paper.

2. MATHEMATICAL MODEL FORMULATION

2.1. The modified mathematical model

In this subsection, we modify the existing SEIR model to study the transmission dynamics of COVID-19 infection in a population. The model is a modification of what is presented in [Alemneh and Telahun \(2020\)](#). In the present model we extended SEIR model by including protected and hospitalized classes

2.2. Model formulation

We formulate a mathematical model to investigate coronavirus diseases (COVID-19) transmission in the presence of protected and hospitalized classes. The model divides the total population into six sub-classes according to their disease status. Susceptible (S), protected (P), exposed (E), infected (I), hospitalized (H) and recovered (R).

The following assumptions have been used in the formulation of the model:

1. The population under study is heterogeneous and varying with time.
2. All recruited human population is susceptible.
3. Susceptible individuals who keeping social distancing, using an alcohol-based hand sanitizer and wearing face masks progress into protected class.
4. Protected individuals cannot acquire infection of COVID-19 disease due to proper use of an alcohol-based hand sanitizer, wearing face masks and keeping social distancing.
5. The latently infected individuals (exposed) could infect other people with a

higher probability than people in the infected class. Since exposed individuals show no symptoms and can easily spread the infection to other people with close contact, often in an unconscious manner.

6. Transmission through human-to-human route is alone considered. Other means of transmission are ignored.
7. We assume that individuals have no permanent immunity after recovery from the disease, that is the recovered individuals have a chance to be susceptible again.
8. The natural mortality rates are assumed to be the same for all the compartments.
9. All parameters in the model being non-negative.

We consider the force of infection λ which is given by

$$\lambda = \beta(\sigma_1 I + \sigma_2 E + \sigma_3 H), \quad (1)$$

where β is the effective contact rate, while σ_1 , σ_2 and σ_3 are the relative infectiousness parameters associated with the infected, exposed and hospitalized classes respectively.

Table 1: The state variables and their descriptions.

Variables	Description of the state variables
S	Susceptible individuals
P	Protected individuals, who keeping social distancing, using an alcohol-based hand sanitizer and wearing face masks properly to protect themselves from the virus
E	Latently infected individuals, who have no symptoms of COVID-19 virus disease but are capable of infecting others
I	Infected individuals, who have active COVID-19 virus disease and can infect other people
H	Hospitalized individuals, who are admitted to health care facility or isolated in their home due to virus infection active cases
R	Recovered individuals

The flow chart of the modified model is illustrated in Figure (1).

Table 2: Parameters of the modified model and their descriptions.

Parameter	Description of the parameter
Π	Recruitment rate of susceptible
θ	Protection rate of susceptible individuals
ν	Waning rate of protected individuals to susceptible class
β	Effective contact rate
σ_1	Modification parameter for relative infectiousness of infected individuals
σ_2	Modification parameter for relative infectiousness of exposed individuals
σ_3	Modification parameter for relative infectiousness of hospitalized individuals
δ	The exposed progression rate
τ	Proportion of exposed individuals who join infected class
$1 - \tau$	The progression from exposed individuals to recovered class
α	Hospitalization rate of infected individuals
μ	Natural death rate
ρ	Disease-induced death rate of infected individuals
ξ	Disease-induced death rate of hospitalized individuals
ε	Rate of recovery of the individuals from infected class
γ	Recovery rate of hospitalized patients
ω	Waning immunity rate
η	The proportion of recovered individuals that become susceptible
$1 - \eta$	The progression from recovered individuals to protected class

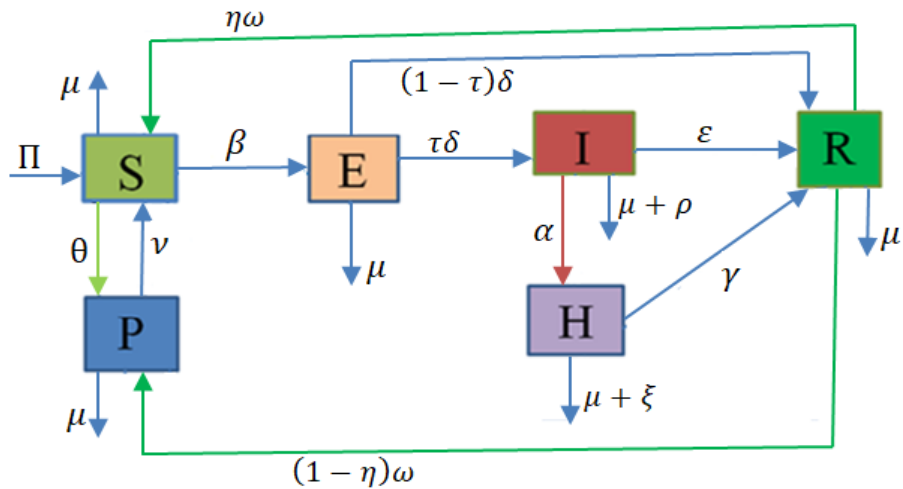


Figure 1: The flow chart for the modified model of COVID-19 pandemic.

Based on our assumptions and the flow chart (1), the modified model for the transmission dynamics of COVID-19 is given by the following deterministic system of non-linear differential equations:

$$\frac{dS}{dt} = \Pi + \eta\omega R + \nu P - \beta(\sigma_1 I + \sigma_2 E + \sigma_3 H)S - (\theta + \mu)S, \quad (2a)$$

$$\frac{dP}{dt} = \theta S + (1 - \eta)\omega R - (\nu + \mu)P, \quad (2b)$$

$$\frac{dE}{dt} = \beta(\sigma_1 I + \sigma_2 E + \sigma_3 H)S - (\delta + \mu)E, \quad (2c)$$

$$\frac{dI}{dt} = \tau\delta E - (\alpha + \varepsilon + \mu + \rho)I, \quad (2d)$$

$$\frac{dH}{dt} = \alpha I - (\gamma + \mu + \xi)H, \quad (2e)$$

$$\frac{dR}{dt} = (1 - \tau)\delta E + \varepsilon I + \gamma H - (\omega + \mu)R, \quad (2f)$$

with non-negative initial conditions $S(0) = S_0 > 0$, $P(0) = P_0 \geq 0$, $E(0) = E_0 \geq 0$, $I(0) = I_0 \geq 0$, $H(0) = H_0 \geq 0$ and $R(0) = R_0 \geq 0$.

3. QUALITATIVE ANALYSIS OF THE MODIFIED MODEL

In this section, we present some basic qualitative properties of the modified model. These analysis include finding the set inside which the model can be sufficiently studied (i.e., the invariant region); local and global stability of equilibrium points of the model (2).

3.1. Well-posedness

Since all the functions on the right hand side of the system (2) are continuously differentiable. Thus, the existence and uniqueness of the solutions is established by the Picard's theorem Valcher (2002). Now, we show the positivity and boundedness of solutions.

Theorem 3.1. (Positivity)

If $S(0) > 0$, $P(0) \geq 0$, $E(0) \geq 0$, $I(0) \geq 0$, $H(0) \geq 0$ and $R(0) \geq 0$, then the solution $(S(t), P(t), E(t), I(t), H(t), R(t))$ of the dynamical system (2) is non-negative for all time $t \geq 0$.

Proof. To show the positivity of the solution of the dynamical system (2), we will perform the proof by using contradiction. We assume that

$S(t) \leq 0$ for some $t \geq 0$, that is there exists small $t_0 > 0$ such that $S(t_0) = 0$, $S'(t_0) \leq 0$ and $S(t) > 0$ for $t \in [0, t_0)$. Then $P(t) \geq 0$, $E(t) \geq 0$ and $I(t) \geq 0$ for $t \in [0, t_0]$. If this be not the case, there exists

Option-I: $t_1 \in [0, t_0]$ such that $P(t_1) = 0$, $P'(t_1) < 0$ and $P(t) > 0$ for $t \in [0, t_1)$. Then $E(t) \geq 0$ and $I(t) \geq 0$ for $t \in [0, t_1]$.

Option-II: $t_2 \in [0, t_1]$ such that $E(t_2) = 0$, $E'(t_2) < 0$ and $E(t) > 0$ for $t \in [0, t_2)$. Then $P(t) \geq 0$ and $I(t) \geq 0$ for $t \in [0, t_2]$.

Option-III: $t_3 \in [0, t_2]$ such that $I(t_3) = 0$, $I'(t_3) < 0$ and $I(t) > 0$ for $t \in [0, t_3)$. Then $P(t) \geq 0$ and $E(t) \geq 0$ for $t \in [0, t_3]$.

It follows from equation (2d) that we have

$$I'(t_3) = \tau\delta E(t_3) - (\alpha + \varepsilon + \mu + \rho)I(t_3).$$

This implies that $I'(t_3) = \tau\delta E(t_3) \geq 0$. This is a contradiction. Integration of equation (2e) leads to

$$H(t) = e^{-(\gamma+\mu+\xi)t} \left(H(0) + \alpha \int_0^t I(s)e^{(\gamma+\mu+\xi)s} ds \right) \geq 0, \quad \text{for } t \in [0, t_2].$$

Then $E'(t_2) = \beta(\sigma_1 I(t_2) + \sigma_3 H(t_2))S(t_2) \geq 0$. This is a contradiction. Hence $H(t) \geq 0$ for every $t \in [0, t_1]$. Integration of equation (2f) leads to

$$R(t) = e^{-(\omega+\mu)t} \left(R(0) + \int_0^t ((1-\tau)\delta E(s) + \varepsilon I(s) + \gamma H(s)) e^{(\omega+\mu)s} ds \right) \geq 0,$$

for $t \in [0, t_1]$.

Then $P'(t_1) = \theta S(t_1) + (1-\eta)\omega R(t_1) \geq 0$. This is a contradiction. Hence $R(t) \geq 0$ for every $t \in [0, t_0]$. Thus $S'(t_0) = \Pi + \eta\omega R(t_0) + \nu P(t_0) > 0$, but this leads to a contradiction to the assumption that $S'(t_0) \leq 0$. Therefore, the solutions $S(t), P(t), E(t), I(t), H(t), R(t)$ in the system (2) remain positive for all $t > 0$. This completes the proof. \square

Theorem 3.2. (Boundedness)

There exists a positively invariant region Ω in which the solution $(S(t), P(t), E(t), I(t), H(t), R(t))$ of the dynamical system (2) is bounded.

Proof. The positivity has already been established by Theorem (3.1). For this model the total population is $N(t) = S(t) + P(t) + E(t) + I(t) + H(t) + R(t)$. Then, we obtain:

$$\frac{dN}{dt} = \Pi - \mu N - (\rho I + \xi H).$$

This implies that

$$\frac{dN}{dt} \leq \Pi - \mu N,$$

Since the solution $I(t)$ and $H(t)$ are positive. Solving the differential inequality we get the relation,

$$N(t) \leq \frac{\Pi}{\mu} + \left(N(0) - \frac{\Pi}{\mu} \right) e^{-\mu t},$$

The existence of the endemic equilibrium point depends on the basic reproduction number R_0 and will be presented later.

If $N(0) \leq \frac{\Pi}{\mu}$, then we obtain $0 \leq N(t) \leq \frac{\Pi}{\mu}$, for all $t \geq 0$. If $N(0) \geq \frac{\Pi}{\mu}$, then we have $0 \leq N(t) \leq N(0)$, for all $t \geq 0$. Thus, the feasible solution set of the system (2) remain in the region

$$\Omega = \left\{ (S, P, E, I, H, R) \in \mathbb{R}_+^6 : 0 \leq N(t) \leq \max \left(N(0), \frac{\Pi}{\mu} \right) \right\}.$$

If we start with initial data $N(0) \in \Omega$, then the solution $N(t) \in \Omega$, for every $t > 0$. This shows the positively invariance of Ω . Thus, the solution of the dynamical system (2) is bounded. \square

3.2. Steady state

The steady states of the system (2) are solutions of the following equations:

$$\begin{aligned} 0 &= \Pi + \eta\omega R + \nu P - \beta(\sigma_1 I + \sigma_2 E + \sigma_3 H)S - (\theta + \mu)S \\ 0 &= \theta S + (1-\eta)\omega R - (\nu + \mu)P \\ 0 &= \beta(\sigma_1 I + \sigma_2 E + \sigma_3 H)S - (\delta + \mu)E \\ 0 &= \tau\delta E - (\alpha + \varepsilon + \mu + \rho)I \\ 0 &= \alpha I - (\gamma + \mu + \xi)H \\ 0 &= (1-\tau)\delta E + \varepsilon I + \gamma H - (\omega + \mu)R. \end{aligned}$$

There are at most two steady states for the system (2): the disease free equilibrium e_0 and endemic equilibrium e_1 . The disease-free equilibrium point of our model is obtained by setting the disease state variables $E = 0, I = 0$ and $H = 0$. Thus, the disease free equilibrium point is given by

$$e_0 = (S^0, P^0, E^0, I^0, H^0, R^0) = \left(\frac{\Pi(\nu + \mu)}{\mu(\theta + \nu + \mu)}, \frac{\Pi\theta}{\mu(\theta + \nu + \mu)}, 0, 0, 0, 0 \right).$$

3.3. Basic reproduction number

The basic reproduction number, which is denoted by R_0 , and defined as the average number of secondary infections produced by a single infected individual in a completely sus-

ceptible population. Using the next generation matrix method [Diekmann et al. \(2010\)](#), the basic reproduction number R_0 can be calculated from the relation $R_0 = \rho(FV^{-1})$. Let

$$\mathcal{F}(x) = \begin{bmatrix} \beta(\sigma_1 I + \sigma_2 E + \sigma_3 H)S \\ 0 \\ 0 \end{bmatrix} \quad \text{and} \quad \mathcal{V}(x) = \begin{bmatrix} (\delta + \mu)E \\ (\alpha + \varepsilon + \mu + \rho)I - \tau\delta E \\ (\gamma + \mu + \xi)H - \alpha I \end{bmatrix}.$$

The Jacobian matrix to \mathcal{F} and \mathcal{V} are

$$F = \left[\frac{\partial \mathcal{F}_i(e_0)}{\partial x_j} \right] = \begin{bmatrix} \beta\sigma_2 S^0 & \beta\sigma_1 S^0 & \beta\sigma_3 S^0 \\ 0 & 0 & 0 \\ 0 & 0 & 0 \end{bmatrix},$$

$$V = \left[\frac{\partial \mathcal{V}_i(e_0)}{\partial x_j} \right] = \begin{bmatrix} \delta + \mu & 0 & 0 \\ -\tau\delta & k_1 & 0 \\ 0 & -\alpha & k_2 \end{bmatrix},$$

where $k_1 = \alpha + \varepsilon + \mu + \rho$ and $k_2 = \gamma + \mu + \xi$. The next-generation matrix FV^{-1} is given by

$$FV^{-1} = \begin{bmatrix} R_1 + R_2 + R_3 & \frac{\beta S^0(\sigma_1 k_2 + \sigma_3 \alpha)}{k_1 k_2} & \frac{\beta \sigma_3 S^0}{k_2} \\ 0 & 0 & 0 \\ 0 & 0 & 0 \end{bmatrix},$$

where

$$R_1 = \frac{\beta\sigma_2 S^0}{\delta + \mu}, \quad R_2 = \frac{\beta\sigma_1 S^0 \tau \delta}{k_1(\delta + \mu)} \quad \text{and} \quad R_3 = \frac{\beta\sigma_3 S^0 \tau \delta \alpha}{k_1 k_2(\delta + \mu)}. \quad (3)$$

$$R_0 = \frac{\Pi\beta(\nu + \mu)}{\mu(\theta + \nu + \mu)(\delta + \mu)} \left(\sigma_2 + \frac{\sigma_1 \tau \delta}{\alpha + \varepsilon + \mu + \rho} + \frac{\sigma_3 \tau \delta \alpha}{(\alpha + \varepsilon + \mu + \rho)(\gamma + \mu + \xi)} \right). \quad (4)$$

3.4. Local stability of disease free equilibrium

Theorem 3.3. The disease free equilibrium point e_0 of the system (2) is locally asymptotically stable if $R_0 < 1$ and unstable if $R_0 > 1$.

Proof. The Jacobian matrix of the system (2) at the disease-free equilibrium e_0 is given by

$$J(e_0) = \left[\begin{array}{cc|ccc} -(\theta + \mu) & \nu & -\beta\sigma_2 S^0 & -\beta\sigma_1 S^0 & -\beta\sigma_3 S^0 & \eta\omega \\ \theta & -(\nu + \mu) & 0 & 0 & 0 & (1 - \eta)\omega \\ \hline 0 & 0 & \beta\sigma_2 S^0 - (\delta + \mu) & \beta\sigma_1 S^0 & \beta\sigma_3 S^0 & 0 \\ 0 & 0 & \tau\delta & -k_1 & 0 & 0 \\ 0 & 0 & 0 & \alpha & -k_2 & 0 \\ 0 & 0 & (1 - \tau)\delta & \varepsilon & \gamma & -(\omega + \mu) \end{array} \right].$$

\mathcal{F} be the vector for the newly infected and \mathcal{V} be the vector for the transfer of individuals into and out of the infected compartments. Let $x = (E, I, H)$, then we obtain:

We find the eigenvalues of FV^{-1} by solving the characteristic equation $|FV^{-1} - \lambda I| = 0$ as $\lambda_1 = R_1 + R_2 + R_3$, $\lambda_2 = 0$ and $\lambda_3 = 0$. The basic reproduction number R_0 is the spectral radius (the largest eigenvalues in modulus) of FV^{-1} which is given by

$$R_0 = \rho(FV^{-1}) = R_1 + R_2 + R_3.$$

The parts R_1 , R_2 and R_3 represent the contributions from the human-to-human transmission routes (exposed-to-susceptible, infected-to-susceptible and hospitalized-to-susceptible individuals, respectively). We can rewrite the basic reproduction number as follows:

The matrix $J(e_0)$ is an upper triangular block matrix. Its eigenvalues are $\lambda_1, \lambda_2, \lambda_3, \lambda_4, \lambda_5$ and λ_6 . Where λ_1, λ_2 are eigenvalues of the first block matrix of $J(e_0)$

and $\lambda_3, \lambda_4, \lambda_5, \lambda_6$ are eigenvalues of the fourth block matrix of $J(e_0)$. The first block matrix of $J(e_0)$ given by

$$J_1(e_0) = \begin{bmatrix} -(\theta + \mu) & \nu \\ \theta & -(\nu + \mu) \end{bmatrix}.$$

We find the eigenvalues of $J_1(e_0)$ by solving the characteristic equation $|J_1(e_0) - \lambda I| = 0$ as

$\lambda_1 = -\mu$ and $\lambda_2 = -(\theta + \nu + \mu)$.
The fourth block matrix of $J(e_0)$ is given by

$$J_4(e_0) = \begin{bmatrix} \beta\sigma_2 S^0 - (\delta + \mu) & \beta\sigma_1 S^0 & \beta\sigma_3 S^0 & 0 \\ \tau\delta & -k_1 & 0 & 0 \\ 0 & \alpha & -k_2 & 0 \\ (1 - \tau)\delta & \varepsilon & \gamma & -(\omega + \mu) \end{bmatrix}.$$

Thus the eigenvalues $\lambda_3, \lambda_4, \lambda_5, \lambda_6$ are obtained from the characteristic equation of $J_4(e_0)$:

$$(-(\omega + \mu) - \lambda)[\lambda^3 + ((\delta + \mu)(1 - R_1) + k_1 + k_2)\lambda^2 + [k_1(\delta + \mu)(1 - (R_1 + R_2)) + k_2(\delta + \mu)(1 - R_1) + k_1 k_2]\lambda + k_1 k_2(\delta + \mu)(1 - R_0)] = 0.$$

From this equation, we obtain the values for λ to be $\lambda_3 = -(\omega + \mu)$ and the eigenvalues $\lambda_4, \lambda_5, \lambda_6$ are the roots of the cubic polynomial:

$$p(\lambda) = a_0\lambda^3 + a_1\lambda^2 + a_2\lambda + a_3 = 0,$$

where

$$\begin{aligned} a_0 &= 1, \\ a_1 &= (\delta + \mu)(1 - R_1) + k_1 + k_2, \\ a_2 &= k_1(\delta + \mu)(1 - (R_1 + R_2)) + k_2(\delta + \mu)(1 - R_1) + k_1 k_2, \\ a_3 &= k_1 k_2(\delta + \mu)(1 - R_0). \end{aligned}$$

Furthermore,

$$\begin{aligned} a_1 a_2 - a_3 &= k_1(\delta + \mu)^2(1 - R_1)(1 - (R_1 + R_2)) + k_2(\delta + \mu)^2(1 - R_1)^2 + k_1 k_2(\delta + \mu)(1 - R_1) \\ &\quad + k_1^2(\delta + \mu)(1 - R_0) + k_1(k_1 + k_2)[k_1(\delta + \mu)R_3 + k_2(\delta + \mu)(1 - R_1) + k_1 k_2]. \end{aligned}$$

If $R_0 < 1$, then R_1, R_2, R_3 and $R_1 + R_2$ are strictly less than one. Since $R_0 = R_1 + R_2 + R_3$. The coefficients a_1, a_2 and a_3 are positive and $a_1 a_2 > a_3$ if $R_0 < 1$. Thus, all the eigenvalues of $J(e_0)$ are negative. It follows by

Routh-Hurwitz criteria that the disease free equilibrium e_0 is locally asymptotically stable for $R_0 < 1$. If $R_0 > 1$, then a_3 is negative and the Routh-Hurwitz criterion tells that the disease free equilibrium e_0 is unstable.

□

3.5. Global stability of disease free equilibrium

Theorem 3.4. For $R_0 < 1$, the disease free equilibrium e_0 of the system (2) is globally asymptotically stable if $S^0 \geq S$.

Proof. Let us rewrite our model system (2) as

$$\begin{aligned} \frac{dZ_1}{dt} &= F(Z_1, Z_2), \\ \frac{dZ_2}{dt} &= G(Z_1, Z_2), \quad G(Z_1, 0) = 0. \end{aligned}$$

Where $Z_1 = (S, P, R) \in \mathbb{R}_+^3$ represents the class of uninfected individuals and $Z_2 = (E, I, H) \in \mathbb{R}_+^3$ represents the class of infected individuals. The disease free equilibrium point of the model is denoted by $U_0 = (Z_1^*, 0)$, where

$Z_1^* = \left(\frac{\Pi(\nu+\mu)}{\mu(\theta+\nu+\mu)}, \frac{\Pi\theta}{\mu(\theta+\nu+\mu)}, 0 \right)$. Since the disease free equilibrium point is locally asymptotically stable (see theorem (3.3)), to prove global stability, we will apply the Castillo-Chavez theorem Castillo-Chavez et al. (2002). From system (2), we have

$$\begin{aligned} \frac{dZ_1}{dt} = F(Z_1, Z_2) &= \begin{bmatrix} \Pi + \eta\omega R + \nu P - \beta(\sigma_1 I + \sigma_2 E + \sigma_3 H)S - (\theta + \mu)S \\ \theta S + (1 - \eta)\omega R - (\nu + \mu)P \\ (1 - \tau)\delta E + \varepsilon I + \gamma H - (\omega + \mu)R \end{bmatrix}, \\ \frac{dZ_2}{dt} = G(Z_1, Z_2) &= \begin{bmatrix} \beta(\sigma_1 I + \sigma_2 E + \sigma_3 H)S - (\delta + \mu)E \\ \tau\delta E - (\alpha + \varepsilon + \mu + \rho)I \\ \alpha I - (\gamma + \mu + \xi)H \end{bmatrix}. \end{aligned}$$

- I. To show Z_1^* is globally asymptotically stable for the system $\frac{dZ_1}{dt} = F(Z_1, 0)$, let us consider the reduced system

$$\frac{dZ_1}{dt} = F(Z_1, 0) = \begin{bmatrix} \Pi + \eta\omega R + \nu P - (\theta + \mu)S \\ \theta S + (1 - \eta)\omega R - (\nu + \mu)P \\ -(\omega + \mu)R \end{bmatrix}. \quad (5)$$

We can rewrite the system (5) as:

$$\frac{dS}{dt} = -(\theta + \mu)S + \nu P + \eta\omega R + \Pi, \quad (61)$$

$$\frac{dP}{dt} = \theta S - (\nu + \mu)P + (1 - \eta)\omega R, \quad (62)$$

$$\frac{dR}{dt} = -(\omega + \mu)R, \quad (63)$$

and admits as solutions

$$\begin{aligned}
 S(t) &= \frac{\Pi(\nu + \mu)}{\mu(\theta + \nu + \mu)} + \frac{1}{\theta + \nu} \left[\left(\nu(S(0) + P(0) + R(0)) - \frac{\Pi\nu}{\mu} \right) e^{-\mu t} \right. \\
 &\quad \left. + \left(\theta S(0) - \nu P(0) + \frac{\omega(\nu - \eta(\theta + \nu))}{\theta + \nu - \omega} R(0) - \frac{\Pi\theta}{\theta + \nu + \mu} \right) e^{-(\theta + \nu + \mu)t} \right] \\
 &\quad - \frac{(\nu - \eta\omega)}{\theta + \nu - \omega} R(0) e^{-(\omega + \mu)t}, \\
 P(t) &= \frac{\Pi\theta}{\mu(\theta + \nu + \mu)} + \frac{1}{\theta + \nu} \left[\left(\theta(S(0) + P(0) + R(0)) - \frac{\Pi\theta}{\mu} \right) e^{-\mu t} \right. \\
 &\quad \left. - \left(\theta S(0) - \nu P(0) + \frac{\omega(\nu - \eta(\theta + \nu))}{\theta + \nu - \omega} R(0) - \frac{\Pi\theta}{\theta + \nu + \mu} \right) e^{-(\theta + \nu + \mu)t} \right] \\
 &\quad - \frac{(\theta - (1 - \eta)\omega)}{\theta + \nu - \omega} R(0) e^{-(\omega + \mu)t}, \\
 R(t) &= R(0) e^{-(\omega + \mu)t}.
 \end{aligned}$$

Taking the limit as t goes to ∞ , we obtain

$$(S(t), P(t), R(t)) \rightarrow \left(\frac{\Pi(\nu + \mu)}{\mu(\theta + \nu + \mu)}, \frac{\Pi\theta}{\mu(\theta + \nu + \mu)}, 0 \right) = Z_1^*.$$

Therefore, Z_1^* is globally asymptotically stable for the system $\frac{dZ_1}{dt} = F(Z_1, 0)$.

II. We will show that $G(Z_1, Z_2) = AZ_2 - \hat{G}(Z_1, Z_2)$, $\hat{G}(Z_1, Z_2) \geq 0$ for $(Z_1, Z_2) \in \Omega$ where $A = \frac{\partial G}{\partial Z_2}(Z_1^*, 0)$ is a Metzler matrix (the off diagonal elements of A are non-negative) and Ω is the region where the model makes biological sense. Consider a matrix

$$A = \frac{\partial G}{\partial Z_2}(Z_1^*, 0) = \begin{bmatrix} \beta\sigma_2 S^0 - (\delta + \mu) & \beta\sigma_1 S^0 & \beta\sigma_3 S^0 \\ \tau\delta & -(\alpha + \varepsilon + \mu + \rho) & 0 \\ 0 & \alpha & -(\gamma + \mu + \xi) \end{bmatrix}.$$

Hence, A is a Metzler matrix (off diagonal elements are non-negative). Here,

$$\hat{G}(Z_1, Z_2) = AZ_2 - G(Z_1, Z_2).$$

After some simplification, we obtain

$$\hat{G}(Z_1, Z_2) = \begin{bmatrix} \beta\sigma_2 E(S^0 - S) + \beta\sigma_1 I(S^0 - S) + \beta\sigma_3 H(S^0 - S) & & \\ & 0 & \\ & & 0 \end{bmatrix},$$

$$\hat{G}(Z_1, Z_2) = (S^0 - S) \begin{pmatrix} \beta(\sigma_2 E + \sigma_1 I + \sigma_3 H) \\ 0 \\ 0 \end{pmatrix} \geq 0.$$

Therefore by Castillo-Chavez theorem [Castillo-Chavez et al. \(2002\)](#), the disease free equilibrium point e_0 of the system (2) is globally asymptotically stable for $R_0 < 1$. \square

3.6. Endemic equilibrium point

Endemic equilibrium point is a steady state solution where the disease persists in the population. In the presence of disease in the population, there exist an equilibrium point

called endemic equilibrium point denoted by $e_1 = (S^*, P^*, E^*, I^*, H^*, R^*)$. It can be obtained by setting each equation of the system (2) equal to zero. Then we obtained

$$\begin{aligned} S^* &= \frac{S^0}{R_0}, \\ P^* &= \frac{\theta S^0 K + (1 - \eta)\omega\mu\delta(\theta + \nu + \mu)[(1 - \tau)k_1k_2 + \varepsilon\tau k_2 + \gamma\alpha\tau]S^0(R_0 - 1)}{(\nu + \mu)KR_0}, \\ E^* &= \frac{k_1k_2\mu(\omega + \mu)(\theta + \nu + \mu)S^0(R_0 - 1)}{KR_0}, \\ I^* &= \frac{k_2\delta\mu\tau(\omega + \mu)(\theta + \nu + \mu)S^0(R_0 - 1)}{KR_0}, \\ H^* &= \frac{\alpha\delta\mu\tau(\omega + \mu)(\theta + \nu + \mu)S^0(R_0 - 1)}{KR_0}, \\ R^* &= \frac{\delta\mu(\theta + \nu + \mu)[(1 - \tau)k_1k_2 + \varepsilon\tau k_2 + \gamma\alpha\tau]S^0(R_0 - 1)}{KR_0}, \end{aligned}$$

where

$$K = k_1k_2[\mu(\nu + \mu)(\omega + \delta + \mu) + \delta\mu(1 - \eta)\omega] + \omega\delta\tau(\eta\mu + \nu)[\alpha(\mu + \xi) + k_2(\mu + \rho)],$$

provided that $R_0 > 1$. From this we see that for the endemic equilibrium to exist $R_0 > 1$.

Moreover, the force of infection can be updated as

$$\lambda^* = \beta(\sigma_1 I^* + \sigma_2 E^* + \sigma_3 H^*). \tag{7}$$

When we substitute the expression for E^*, I^* and H^* into the force of infection λ^* , we obtain

$$\lambda^* = \frac{\mu k_1 k_2 (\delta + \mu) (\omega + \mu) (\theta + \nu + \mu) (R_0 - 1)}{K}, \tag{8}$$

provided that $R_0 > 1$. From this, we see that, there is no endemic equilibrium of the system (2) if $R_0 < 1$. Therefore, this condition shows that it is not possible for backward bifurcation in this model. Hence we have established the following result.

3.7. Local stability of endemic equilibrium

Theorem 3.6. The endemic equilibrium e_1 of the system (2) is locally asymptotically stable

Theorem 3.5. A unique endemic equilibrium point $e_1 = (S^*, P^*, E^*, I^*, H^*, R^*)$ exists and is positive if $R_0 > 1$.

When we plot the force of infection λ^* over R_0 by using the expression for λ^* we got a forward bifurcation in Figure (2).

if $R_0 > 1$.

Proof. To determine the local stability of endemic equilibrium, we used the center manifold theory [Castillo-Chavez and Song \(2004\)](#), by taking β as a bifurcation parameter. We make the following change of variables on the system (2). Let $S = x_1, P = x_2, E = x_3, I = x_4, H =$

x_5 and $R = x_6$. Moreover, by using vector notation $x = (x_1, x_2, x_3, x_4, x_5, x_6)^T$, the system (2) can be written in the form $\frac{dx}{dt} = F(x)$, with $F = (f_1, f_2, f_3, f_4, f_5, f_6)^T$.

We choose $\beta = \beta^*$ as a bifurcation parameter. Solving for β^* from $R_0 = 1$, we obtain

$$\beta^* = \frac{\mu(\theta + \nu + \mu)(\delta + \mu)(\alpha + \varepsilon + \mu + \rho)(\gamma + \mu + \xi)}{\Pi(\nu + \mu)[\sigma_2(\alpha + \varepsilon + \mu + \rho)(\gamma + \mu + \xi) + \sigma_1\tau\delta(\gamma + \mu + \xi) + \sigma_3\tau\delta\alpha]}.$$

The Jacobian matrix of the system (2) evaluated at the disease free equilibrium e_0 with $\beta = \beta^*$ is given by

$$J^* = \begin{bmatrix} -(\theta + \mu) & \nu & -\beta^*\sigma_2S^0 & -\beta^*\sigma_1S^0 & -\beta^*\sigma_3S^0 & \eta\omega \\ \theta & -(\nu + \mu) & 0 & 0 & 0 & (1 - \eta)\omega \\ 0 & 0 & \beta^*\sigma_2S^0 - (\delta + \mu) & \beta^*\sigma_1S^0 & \beta^*\sigma_3S^0 & 0 \\ 0 & 0 & \tau\delta & -k_1 & 0 & 0 \\ 0 & 0 & 0 & \alpha & -k_2 & 0 \\ 0 & 0 & (1 - \tau)\delta & \varepsilon & \gamma & -(\omega + \mu) \end{bmatrix},$$

where $k_1 = \alpha + \varepsilon + \mu + \rho$, $k_2 = \gamma + \mu + \xi$.

The Jacobian matrix J^* of the linearized system has a simple zero eigenvalue with all other eigenvalues having negative real part, hence the center manifold theory will be used to analyse the dynamics of the sys-

tem near $\beta = \beta^*$. Thus, e_0 is a non-hyperbolic equilibrium, when $\beta = \beta^*$. Now, the components of the right eigenvector $w = (w_1, w_2, w_3, w_4, w_5, w_6)^T$ of J^* associated with the zero eigenvalue are given by

$$\begin{aligned} w_1 &= -\frac{k_1k_2[\mu(\nu + \mu)(\omega + \delta + \mu) + \delta\mu(1 - \eta)\omega] + \omega\delta\tau(\eta\mu + \nu)[\alpha(\mu + \xi) + k_2(\mu + \rho)]}{\tau\delta\mu k_2(\theta + \nu + \mu)(\omega + \mu)}w_4, \\ w_2 &= -\frac{\omega\delta\mu[\tau(k_2(\mu + \rho) + \alpha(\mu + \xi))(2 - \eta) - (1 - \eta)] + \theta\mu(\delta + \omega + \mu)}{\tau\delta\mu k_2(\theta + \nu + \mu)(\omega + \mu)}w_4, \\ w_3 &= \frac{\alpha + \varepsilon + \mu + \rho}{\tau\delta}w_4, \quad w_4 = w_4 > 0, \quad w_5 = \frac{\alpha}{\gamma + \mu + \xi}w_4, \\ w_6 &= \frac{(1 - \tau)(\alpha + \varepsilon + \mu + \rho)(\gamma + \mu + \xi) + \varepsilon\tau(\gamma + \mu + \xi) + \gamma\alpha\tau}{\tau(\omega + \mu)(\gamma + \mu + \xi)}w_4. \end{aligned}$$

Similarly, the components of the left eigenvector $v = (v_1, v_2, v_3, v_4, v_5, v_6)^T$ of J^* associ-

ated with the zero eigenvalue are given by

$$v_1 = v_2 = v_6 = 0, \quad v_3 = v_3 > 0, \quad v_4 = \frac{\beta^*S^0(\sigma_1(\gamma + \mu + \xi) + \alpha\sigma_3)}{(\alpha + \varepsilon + \mu + \rho)(\gamma + \mu + \xi)}v_3, \quad v_5 = \frac{\beta^*S^0\sigma_3}{\gamma + \mu + \xi}v_3.$$

Since the first, second and six component of v are zero, we don't need the partial derivatives of f_1, f_2 and f_6 . From the partial derivatives

of f_3, f_4 and f_5 at the disease free equilibrium point, the only ones that are nonzero are the following:

$$\begin{aligned} \frac{\partial^2 f_3}{\partial x_3 \partial x_1} &= \frac{\partial^2 f_3}{\partial x_1 \partial x_3} = \beta^* \sigma_2, & \frac{\partial^2 f_3}{\partial x_4 \partial x_1} &= \frac{\partial^2 f_3}{\partial x_1 \partial x_4} = \beta^* \sigma_1, & \frac{\partial^2 f_3}{\partial x_5 \partial x_1} &= \frac{\partial^2 f_3}{\partial x_1 \partial x_5} = \beta^* \sigma_3, \\ \frac{\partial^2 f_3}{\partial x_3 \partial \beta} &= \sigma_2 S^0, & \frac{\partial^2 f_3}{\partial x_4 \partial \beta} &= \sigma_1 S^0, & \frac{\partial^2 f_3}{\partial x_5 \partial \beta} &= \sigma_3 S^0. \end{aligned}$$

The direction of the bifurcation at $R_0 = 1$ is determined by the signs of the bifurcation coefficients a and b . Hence,

$$\begin{aligned} a &= v_3 \sum_{i,j=1}^6 w_i w_j \frac{\partial^2 f_3}{\partial x_i \partial x_j} (S^0, P^0, 0, 0, 0, 0) = 2v_3 w_1 (w_3 \beta^* \sigma_2 + w_4 \beta^* \sigma_1 + w_5 \beta^* \sigma_3) \\ &= 2\beta^* w_1 \left(\frac{\sigma_2 k_1}{\tau \delta} + \sigma_1 + \frac{\alpha \sigma_3}{k_2} \right) v_3 w_4 \\ &= - \frac{2(\delta + \mu)}{(\tau \delta)^2 k_2 \Pi(\nu + \mu)(\omega + \mu)} [k_1^2 k_2 (\mu(\nu + \mu)(\omega + \delta + \mu) + \delta \mu(1 - \eta)\omega) \\ &\quad + \omega \delta \tau k_1 (\eta \mu + \nu) (\alpha(\mu + \xi) + k_2(\mu + \rho))] v_3 w_4^2 < 0. \end{aligned}$$

and

$$\begin{aligned} b &= v_3 \sum_{i=1}^6 w_i \frac{\partial^2 f_3}{\partial x_i \partial \beta} (S^0, P^0, 0, 0, 0, 0) = v_3 \left(\frac{k_1 w_4 \sigma_2 S^0}{\tau \delta} + w_4 \sigma_1 S^0 + \frac{\alpha w_4 \sigma_3 S^0}{k_2} \right) \\ &= \frac{(\delta + \mu)(\alpha + \varepsilon + \mu + \rho)}{\beta^* \tau \delta} v_3 w_4 > 0. \end{aligned}$$

Since $a < 0$ and $b > 0$ at $\beta = \beta^*$. Based on the Theorem 4.1 stated in [Castillo-Chavez and Song \(2004\)](#), the system (2) undergoes a for-

ward bifurcation at $R_0 = 1$ and the unique endemic equilibrium e_1 is locally asymptotically stable for $R_0 > 1$.

□

3.8. Bifurcation analysis

We investigate the nature of the bifurcation by using the center manifold theory [Castillo-Chavez and Song \(2004\)](#). In short, the theory is summarized by Theorem 4.1 in [Castillo-Chavez and Song \(2004\)](#). In such a theorem, there are two important quantities: the coefficients, say a and b , of the normal form representing the dynamics of the system on the central manifold. These coefficients decide the bifurcation. In particular, if $a < 0$ and $b > 0$,

then the bifurcation is forward. In the proof of Theorem (3.6), we have already justified the system (2) undergoes a forward bifurcation at $R_0 = 1$. Thus the basic reproduction number R_0 plays an important role in the disease spread. If $R_0 < 1$, then its easy to control the disease but if $R_0 > 1$, then the society will experience endemic disease spreading. The forward bifurcation diagram can be seen in Figure (2).

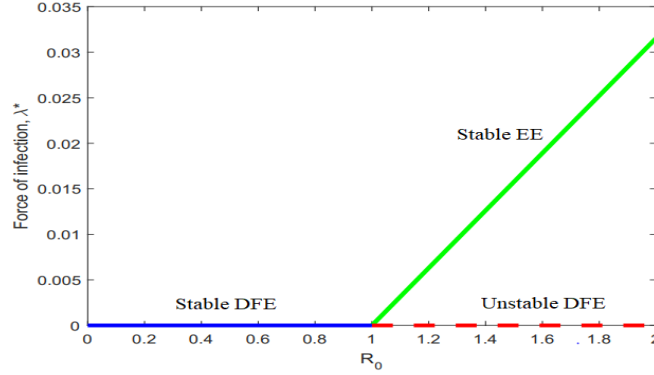


Figure 2: Forward bifurcation diagram for the COVID-19 model (2).

From Figure (2), it is clear that when $R_0 < 1$, the system (2) has no endemic equilibrium and the disease-free equilibrium is stable. When $R_0 > 1$, a stable endemic equilibrium appears and the disease free equilibrium becomes unstable, i.e. exchange of stability of the equilibrium's (forward bifurcation) occurs at the bifurcation point $R_0^* = 1$.

3.9. Sensitivity analysis

Sensitivity analysis is a useful tool in model building as well as in model evaluation by showing how the model behavior responds to changes in parameter values [Martcheva \(2015\)](#). The threshold parameter R_0 which determines stability is a function of the parameters $\Pi, \beta, \sigma_1, \sigma_2, \sigma_3, \nu, \mu, \theta, \delta, \gamma, \xi, \alpha, \varepsilon, \rho, \tau$. We recall that the basic reproduction number R_0 is given by

$$R_0 = \frac{\Pi\beta(\nu + \mu) [(\gamma + \mu + \xi) [\sigma_2(\alpha + \varepsilon + \mu + \rho) + \sigma_1\tau\delta] + \sigma_3\tau\delta\alpha]}{\mu(\theta + \nu + \mu)(\delta + \mu)(\alpha + \varepsilon + \mu + \rho)(\gamma + \mu + \xi)}$$

Thus, in order to identify the most sensitive parameters for model (2), we compute the relative sensitivity of R_0 with respect to the above parameters. Then using the parameter

values from Table (3), we display the sensitivity indices of R_0 with respect to the parameters in Figure (3).

$$\begin{aligned} \Delta_{\beta}^{R_0} &= \frac{\partial R_0}{\partial \beta} \times \frac{\beta}{R_0} = 1, \\ \Delta_{\Pi}^{R_0} &= \frac{\partial R_0}{\partial \Pi} \times \frac{\Pi}{R_0} = 1, \\ \Delta_{\sigma_1}^{R_0} &= \frac{\partial R_0}{\partial \sigma_1} \times \frac{\sigma_1}{R_0} = \frac{\sigma_1 \tau \delta (\gamma + \mu + \xi)}{(\gamma + \mu + \xi) [\sigma_2 (\alpha + \varepsilon + \mu + \rho) + \sigma_1 \tau \delta] + \sigma_3 \tau \delta \alpha}, \\ \Delta_{\sigma_2}^{R_0} &= \frac{\partial R_0}{\partial \sigma_2} \times \frac{\sigma_2}{R_0} = \frac{\sigma_2 (\alpha + \varepsilon + \mu + \rho) (\gamma + \mu + \xi)}{(\gamma + \mu + \xi) [\sigma_2 (\alpha + \varepsilon + \mu + \rho) + \sigma_1 \tau \delta] + \sigma_3 \tau \delta \alpha}, \\ \Delta_{\sigma_3}^{R_0} &= \frac{\partial R_0}{\partial \sigma_3} \times \frac{\sigma_3}{R_0} = \frac{\sigma_3 \tau \delta \alpha}{(\gamma + \mu + \xi) [\sigma_2 (\alpha + \varepsilon + \mu + \rho) + \sigma_1 \tau \delta] + \sigma_3 \tau \delta \alpha}, \\ \Delta_{\tau}^{R_0} &= \frac{\partial R_0}{\partial \tau} \times \frac{\tau}{R_0} = \frac{\tau \delta [\sigma_1 (\gamma + \mu + \xi) + \sigma_3 \alpha]}{(\gamma + \mu + \xi) [\sigma_2 (\alpha + \varepsilon + \mu + \rho) + \sigma_1 \tau \delta] + \sigma_3 \tau \delta \alpha}, \\ \Delta_{\nu}^{R_0} &= \frac{\partial R_0}{\partial \nu} \times \frac{\nu}{R_0} = \frac{\theta \nu}{(\theta + \nu + \mu) (\nu + \mu)}, \\ \Delta_{\alpha}^{R_0} &= \frac{\partial R_0}{\partial \alpha} \times \frac{\alpha}{R_0} = \frac{\alpha \tau \delta [\sigma_3 (\varepsilon + \mu + \rho) - \sigma_1 (\gamma + \mu + \xi)]}{(\alpha + \varepsilon + \mu + \rho) [(\gamma + \mu + \xi) [\sigma_2 (\alpha + \varepsilon + \mu + \rho) + \sigma_1 \tau \delta] + \sigma_3 \tau \delta \alpha]}, \\ \Delta_{\delta}^{R_0} &= \frac{\partial R_0}{\partial \delta} \times \frac{\delta}{R_0} = \frac{\delta [(\gamma + \mu + \xi) [\sigma_1 \tau \mu - \sigma_2 (\alpha + \varepsilon + \mu + \rho)] + \sigma_3 \tau \alpha \mu]}{(\delta + \mu) [(\gamma + \mu + \xi) [\sigma_2 (\alpha + \varepsilon + \mu + \rho) + \sigma_1 \tau \delta] + \sigma_3 \tau \delta \alpha]}, \\ \Delta_{\theta}^{R_0} &= \frac{\partial R_0}{\partial \theta} \times \frac{\theta}{R_0} = -\frac{\theta}{\theta + \nu + \mu}, \\ \Delta_{\varepsilon}^{R_0} &= \frac{\partial R_0}{\partial \varepsilon} \times \frac{\varepsilon}{R_0} = -\frac{\varepsilon \tau \delta [\sigma_1 (\gamma + \mu + \xi) + \sigma_3 \alpha]}{(\alpha + \varepsilon + \mu + \rho) [(\gamma + \mu + \xi) [\sigma_2 (\alpha + \varepsilon + \mu + \rho) + \sigma_1 \tau \delta] + \sigma_3 \tau \delta \alpha]}, \\ \Delta_{\rho}^{R_0} &= \frac{\partial R_0}{\partial \rho} \times \frac{\rho}{R_0} = -\frac{\rho \tau \delta [\sigma_1 (\gamma + \mu + \xi) + \sigma_3 \alpha]}{(\alpha + \varepsilon + \mu + \rho) [(\gamma + \mu + \xi) [\sigma_2 (\alpha + \varepsilon + \mu + \rho) + \sigma_1 \tau \delta] + \sigma_3 \tau \delta \alpha]}, \\ \Delta_{\gamma}^{R_0} &= \frac{\partial R_0}{\partial \gamma} \times \frac{\gamma}{R_0} = -\frac{\sigma_3 \tau \delta \alpha \gamma}{(\gamma + \mu + \xi) [(\gamma + \mu + \xi) [\sigma_2 (\alpha + \varepsilon + \mu + \rho) + \sigma_1 \tau \delta] + \sigma_3 \tau \delta \alpha]}, \\ \Delta_{\xi}^{R_0} &= \frac{\partial R_0}{\partial \xi} \times \frac{\xi}{R_0} = -\frac{\sigma_3 \tau \delta \alpha \xi}{(\gamma + \mu + \xi) [(\gamma + \mu + \xi) [\sigma_2 (\alpha + \varepsilon + \mu + \rho) + \sigma_1 \tau \delta] + \sigma_3 \tau \delta \alpha]}, \\ \Delta_{\mu}^{R_0} &= \frac{\partial R_0}{\partial \mu} \times \frac{\mu}{R_0} = \frac{1}{(\nu + \mu) D} [\mu D - [\sigma_2 A (\alpha + \varepsilon + \mu + \rho)^2 (\gamma + \mu + \xi)^2 (\nu + \mu) \\ &\quad + \sigma_1 \tau \delta [(\alpha + \varepsilon + \rho) A + B] (\gamma + \mu + \xi)^2 (\nu + \mu) + \sigma_3 \tau \delta \alpha [(\gamma + \xi) (A + B) \\ &\quad + (\alpha + \varepsilon + \rho) B + C] (\nu + \mu)], \end{aligned}$$

where

$$\begin{aligned} A &= \delta (\theta + \nu) + 2\mu (\delta + \theta + \nu) + 3\mu^2, \quad B = 2\mu \delta (\theta + \nu) + 3\mu^2 (\delta + \theta + \nu) + 4\mu^3, \\ C &= 3\mu^2 \delta (\theta + \nu) + 4\mu (\delta + \theta + \nu) + 5\mu^4, \\ D &= (\alpha + \varepsilon + \mu + \rho) (\gamma + \mu + \xi) (\delta + \mu) (\theta + \nu + \mu) [(\gamma + \mu + \xi) [\sigma_2 (\alpha + \varepsilon + \mu + \rho) + \sigma_1 \tau \delta] \\ &\quad + \sigma_3 \tau \delta \alpha]. \end{aligned}$$

Note that the sensitivity index may depend on several parameters of the system, but also can be constant, independent of any parameter. For example, $\Delta_{\beta}^{R_0} = +1$ means that in-

creasing (decreasing) β by a given percentage increases (decreases) always R_0 by that same percentage.

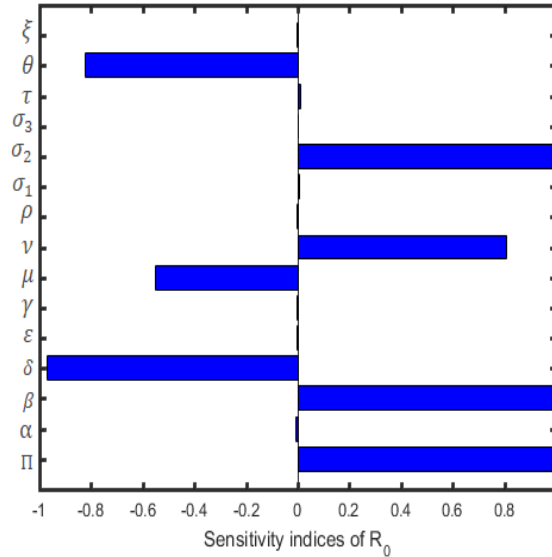


Figure 3: The sensitivity indices of R_0 with respect to the parameters.

Figure (3) shows that the recruitment rate Π , the contact rate β , the modification parameter σ_2 , the exposed progression rate δ , the natural death rate μ , the protection rate θ and the waning rate of protected individuals to susceptible class ν are the most sensitive parameters for R_0 . The parameters $\tau, \sigma_1, \sigma_2, \sigma_3, \nu, \beta$ and Π have positive correlation with R_0 . This indicates that the spread of COVID-19 decreases with decrease of these parameters. The parameters $\xi, \theta, \rho, \mu, \gamma, \epsilon, \delta$ and α have negative correlation with R_0 . This implies that the spread of the virus decreases with an increase of these parameters.

4. NUMERICAL SIMULATIONS AND DISCUSSION

In this section, we perform numerical simulation to support our analytical results. The

numerical simulations are carried out with help of the ode45 Matlab tool. Using the parameter values given in Table (3) and the initial conditions below in the model equations (2) simulation study is conducted. The parameter values have been taken based on the literature and the real characteristics of the virus. Furthermore, initial conditions are determined as follow. The total population of Ethiopia for the year 2021 is estimated about $N(0) = 114,963,588$ people Kifle and Obsu (2022). On December 31, 2020 the total active cases (Infected individuals are 10,245 i.e $I(0) = 10,245$), and the Hospitalized are $H(0) = 5062$ and the total recovered by the date are $R(0) = 81,144$ and we are assumed $P(0) = 108076, E(0) = 15000$ and hence is $S(0) = N(0) - (P(0) + E(0) + I(0) + H(0) + R(0)) = 114,744,061$.

Table 3: The parameter values of the modified model (per day).

Parameter	Value	Source
Π	1300	Assumed
θ	0.7	Assumed
ν	0.15	Assumed
β	0.00000058	Assumed
σ_1	0.0001	Alemneh and Telahun (2020)
σ_2	0.02	Alemneh and Telahun (2020)
σ_3	0.00003	Assumed
δ	1/14	Kifle and Obsu (2022)
α	0.04	Assumed
μ	1/(64*12*30)	Kifle and Obsu (2022)
ρ	0.0004	Alemneh and Telahun (2020)
ξ	0.015	Assumed
τ	0.7	Alemneh and Telahun (2020)
ε	0.0476	Assumed
γ	0.033	Assumed
η	0.4	Assumed
ω	0.011	Assumed

Figure (4) shows the predicted total confirmed cases and the real data total confirmed cases for Ethiopia from 31 December 2020 to 30 March 2022 (It the data has been taken [COVID-19 pandemic \(2022\)](#)). There is some differences between the prediction and the real

data that should come due to the fact that there were no enough covid test kits during the early time not only in Ethiopia but also all over the world. After wards we continue to validate the local stability of DFE and EEP of model.

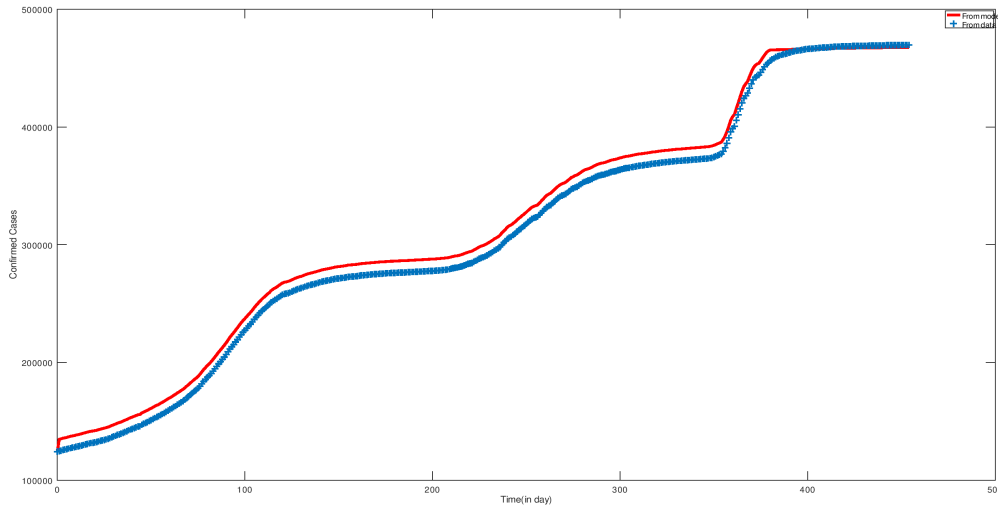


Figure 4: The prediction using model (2) and the real data of confirmed cases for Ethiopia from 31 December 2020 to 30 March 2022

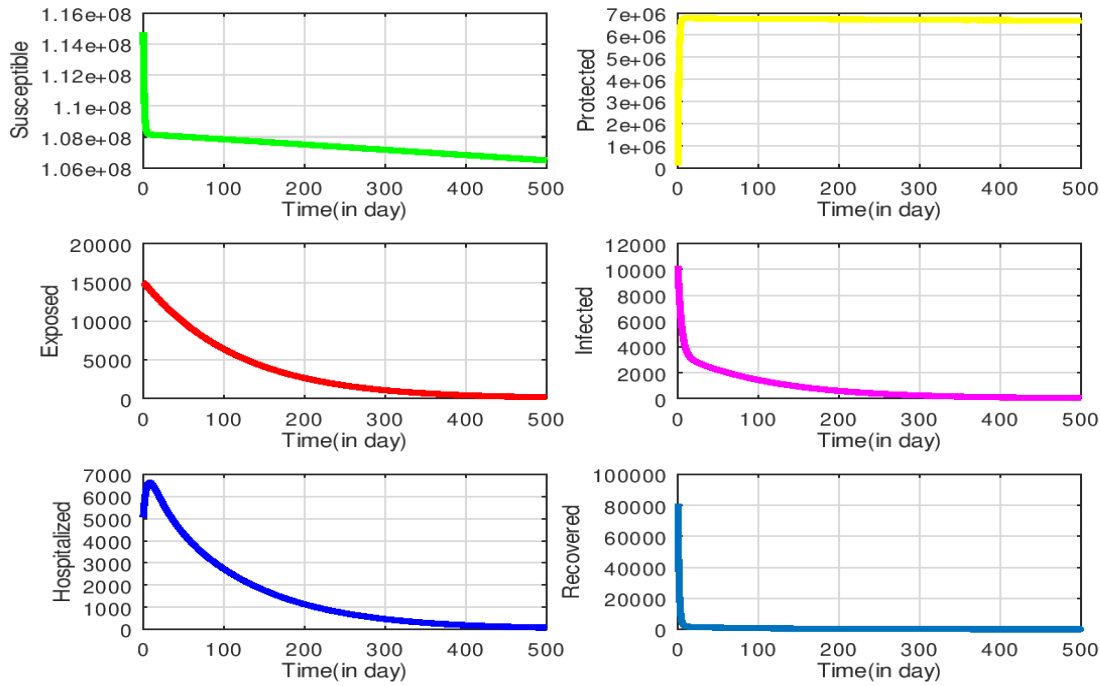
In Figure (5) with $R_0 = 0.22950$, we observe that for the basic reproduction number $R_0 < 1$, all solutions curve goes to the disease free equilibrium point. As a result, the disease goes to extinct or the disease dies out.

In Figure (6) with $R_0 = 1.10791$, we observe that for the basic reproduction number

$R_0 > 1$, all solutions curve goes away from the disease free equilibrium point. These indicate that the disease-free equilibrium point is unstable for the values of $R_0 > 1$, and the solutions will go to the endemic equilibrium point. Consequently, the disease invade in a population.

In Figure (7), we observe as the protection rate θ increases, all infected classes will significantly decrease over time. This confirmed the result from the fact that strict use of safety (protection) measures within the population plays a critical role in confine the spread of

the disease as in [Bachar et al. \(2021\)](#). It is predicted that the population will be disease-free. This is due to the case that when protection rate increases the basic reproduction number decreases.


 Figure 5: The time series plot of model (2) when $R_0 = 0.22950$

In Figure (8), we observe that as the contact rate β decrease, R_0 and also all infected classes are decreasing. Further this habitual the result obtained from the fact that a decrease in contact among the population plays a indispensable role in curtailing the spread of the disease as in [Ahmed et al. \(2021\)](#).

5. EXTENSION OF THE MODIFIED MODEL INTO AN OPTIMAL CONTROL

In this section, we will use optimal control theory to find protection (for susceptible) and hospitalization (for infected) strategies that would mitigate the spread of COVID-19 in the population.

5.1. Optimal protection and hospitalization using modified model

In this subsection, we study the optimal protection of susceptible population and hospitalization of infected individuals in order to minimize the outbreak of COVID-19 in the

population. Let us define our control set U to be

$$U = \{(\theta(t), \alpha(t)) : 0 \leq \theta(t), \alpha(t) \leq \epsilon_i, 0 \leq t \leq T, 0 < \epsilon_i \leq 1, i = 1, 2\} \quad (9)$$

where $\theta(t)$ and $\alpha(t)$ are Lebesgue measurable quantities bounded above by ϵ_1 and ϵ_2 respectively. We will minimize the objective functional

$$\begin{aligned} J[\theta(t), \alpha(t)] &= \int_0^T \left(B_1 E(t) + B_2 I(t) + \frac{1}{2} (A_1 \theta^2(t) + A_2 \alpha^2(t)) \right) dt, \end{aligned} \quad (10)$$

where constants B_1, B_2, A_1 and A_2 are positive. Here, we want to find the optimal values $\theta(t)$ and $\alpha(t)$ that minimizes the objective functional (10) subject to the state system (2).

The goal is to find the optimal control $(\theta^*(t), \alpha^*(t))$ such that

$$J[\theta^*(t), \alpha^*(t)] = \min_{(\theta, \alpha) \in U} J[\theta(t), \alpha(t)]. \quad (11)$$

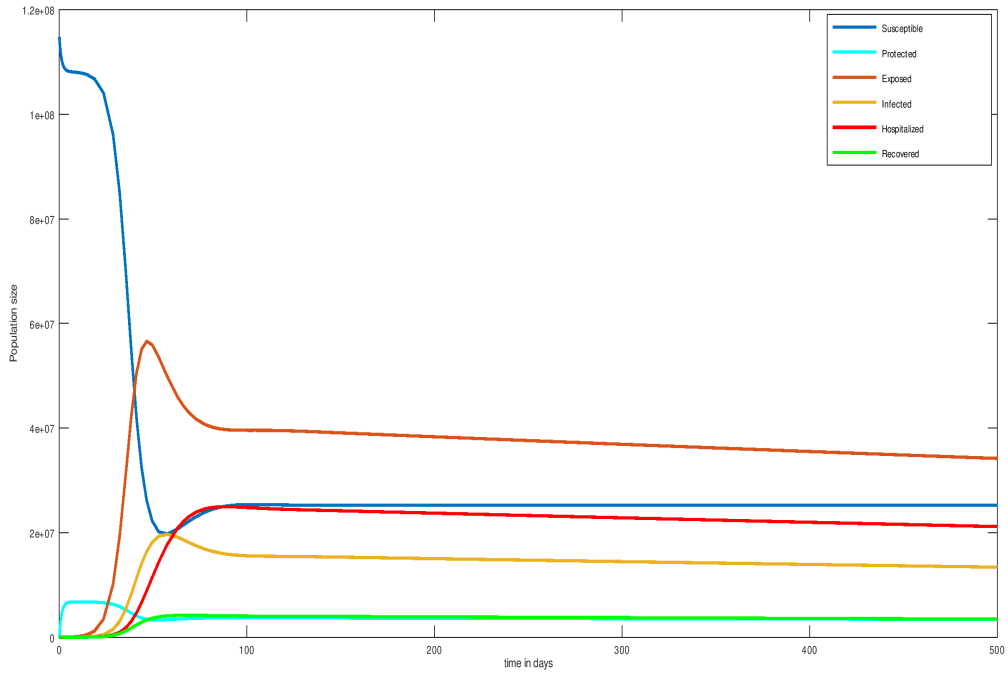


Figure 6: The time series plot of model (2) when $\beta = 0.0000028$ with $R_0 = 1.11073$

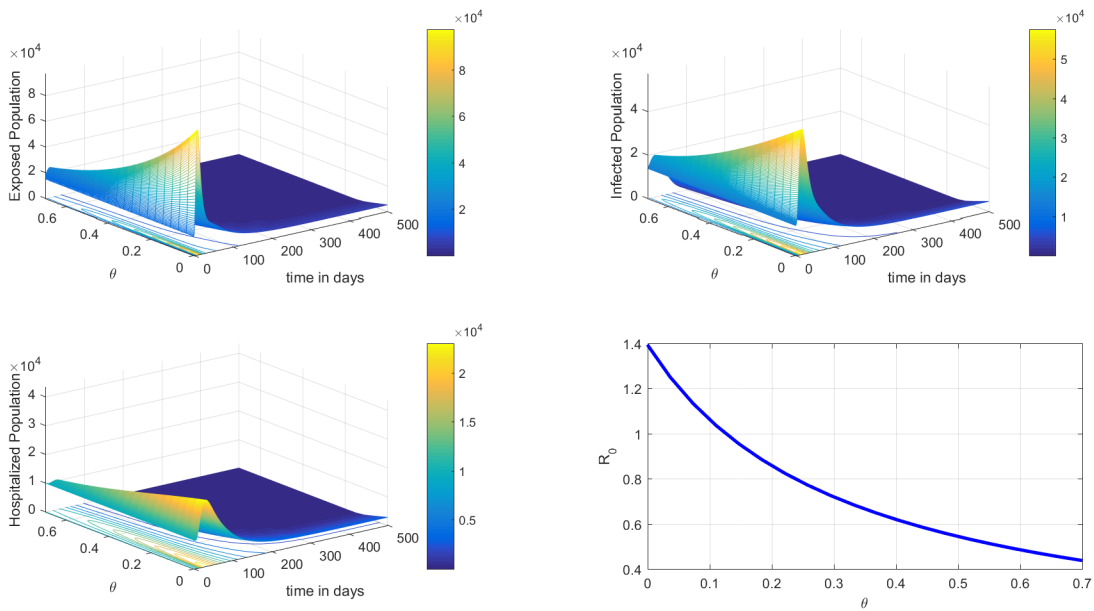
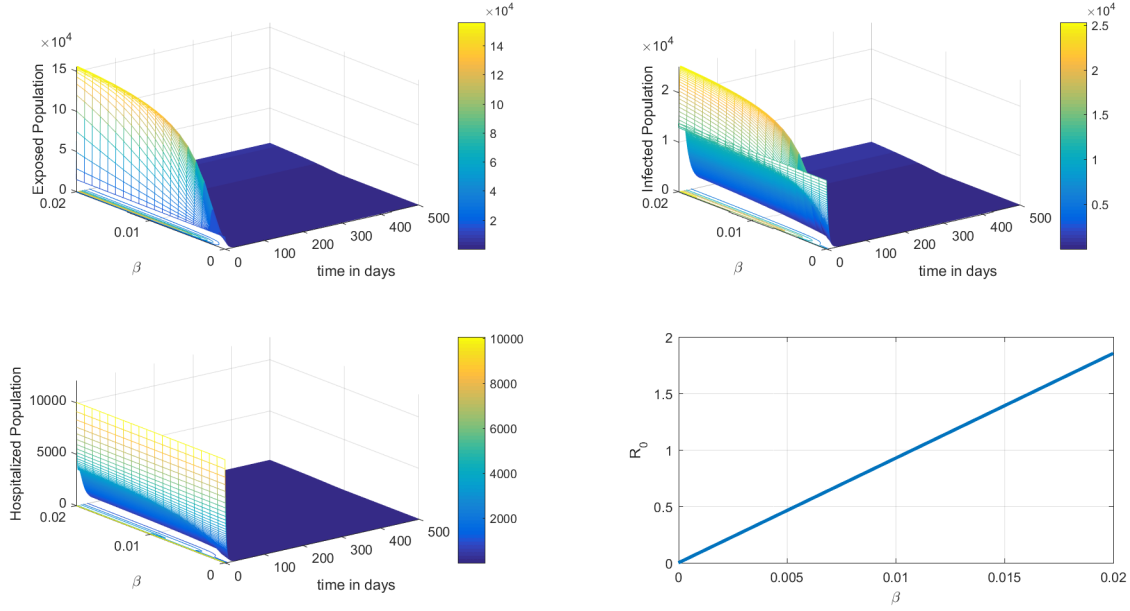


Figure 7: Impact of protection rate θ on R_0 and infected classes.

5.2. Existence of an optimal control

The existence of the optimal control can be showed by using an approach of Fleming and


 Figure 8: Impact of contact rate β on R_0 and infected classes.

Rishel (2012).

Theorem 5.1. Given the objective functional $J(\theta(t), \alpha(t))$ (10) with admissible control set U , subject to the state system (2), then there

Proof. To prove the existence of optimal control, we need to verify the following conditions.

- (a) The set of solutions to the state system (2) and control parameters in (9) are non-empty.
- (b) The set U is convex and closed.
- (c) The right hand side of system (2) is bounded above by sum of bounded control and state and can be written as a linear function of the control variables with coefficients dependent on time and state variables.
- (d) The integrand function $L(E, I, \theta, \alpha, t)$ is convex on U and $L(E, I, \theta, \alpha, t) \geq h(u)$, where $h(u)$ is continuous and $\|u\|^{-1}h(u) \rightarrow \infty$ when $\|u\| \rightarrow \infty$. Here $u = (\theta(t), \alpha(t))$.

exist an optimal control double $u^* = (\theta^*, \alpha^*)$ in U such that

$$J[\theta^*, \alpha^*] = \min_{(\theta, \alpha) \in U} J[\theta(t), \alpha(t)]. \quad (12)$$

In Theorem (3.2), we have already justified the boundedness of the solution of the state system (2). Since our solution for the model is bounded by $N(t) \leq \max\left(N(0), \frac{\Pi}{\mu}\right)$ for all $t \geq 0$. This implies that the solutions of the state system are continuous and bounded for each admissible control functions in U . Moreover, the right hand side of the model equations (2) satisfies the Lipschitz condition with respect to state variables. Hence, the state system (2) has a unique solution corresponding to each admissible control function $(\theta(t), \alpha(t)) \in U$. Thus, condition (a) is achieved.

To verify condition (b), given that the control set $U = \{u \in \mathbb{R}^2 : \|u\|_\infty \leq 1\}$. Let $\psi \in [0, 1]$ and $v_1, v_2 \in U$ such that $\|v_1\|_\infty \leq 1$ and $\|v_2\|_\infty \leq 1$, then

$$\|\psi v_1 + (1-\psi)v_2\|_\infty \leq \psi\|v_1\|_\infty + (1-\psi)\|v_2\|_\infty \leq 1.$$

Thus, the set U is convex and closed.

To verify condition (c), let $u = (\theta(t), \alpha(t)) \in U$, $X = (S, P, E, I, H, R)$ and the right hand side of the state system (2) is given by

$$f(t, X, u) = \begin{bmatrix} \Pi + \eta\omega R + \nu P - \beta(\sigma_1 I + \sigma_2 E + \sigma_3 H)S - (\theta(t) + \mu)S \\ \theta(t)S + (1 - \eta)\omega R - (\nu + \mu)P \\ \beta(\sigma_1 I + \sigma_2 E + \sigma_3 H)S - (\delta + \mu)E \\ \tau\delta E - (\alpha(t) + \varepsilon + \mu + \rho)I \\ \alpha(t)I - (\gamma + \mu + \xi)H \\ (1 - \tau)\delta E + \varepsilon I + \gamma H - (\omega + \mu)R \end{bmatrix}. \quad (13)$$

Then from (13) we get, $f(t, X, u) = g(t, X) + h(t, X)u^T$, where

$$g(t, X) = \begin{bmatrix} \Pi + \eta\omega R + \nu P - \beta(\sigma_1 I + \sigma_2 E + \sigma_3 H)S - \mu S \\ (1 - \eta)\omega R - (\nu + \mu)P \\ \beta(\sigma_1 I + \sigma_2 E + \sigma_3 H)S - (\delta + \mu)E \\ \tau\delta E - (\varepsilon + \mu + \rho)I \\ -(\gamma + \mu + \xi)H \\ (1 - \tau)\delta E + \varepsilon I + \gamma H - (\omega + \mu)R \end{bmatrix} \quad \text{and} \quad h(t, X) = \begin{bmatrix} -S & 0 \\ S & 0 \\ 0 & 0 \\ 0 & -I \\ 0 & I \\ 0 & 0 \end{bmatrix}.$$

Since, by using the properties of a norm of a matrix we have,

$$\|f(t, X, u)\| = \|g(t, X) + h(t, X)u^T\| \leq \|g(t, X)\| + \|h(t, X)\| \|u\|.$$

Thus, condition (c) is proved.

To verify condition (d), the integrand of the objective functional (10)

$$L(E, I, \theta, \alpha, t) = B_1 E(t) + B_2 I(t) + \frac{1}{2} (A_1 \theta^2(t) + A_2 \alpha^2(t)) \quad (14)$$

is the sum of convex function and hence convex with respect to control parameters $\theta(t)$ and $\alpha(t)$. Moreover,

$$L(E, I, \theta, \alpha, t) = B_1 E(t) + B_2 I(t) + \frac{1}{2} (A_1 \theta^2(t) + A_2 \alpha^2(t)) \geq \frac{1}{2} (A_1 \theta^2(t) + A_2 \alpha^2(t)).$$

We define a continuous function $h(u) = \phi \|u\|^2$, where $\phi = \min\left(\frac{A_1}{2}, \frac{A_2}{2}\right) > 0$ and $u = (\theta(t), \alpha(t))$. Then we have

$$L(E, I, \theta, \alpha, t) \geq \frac{1}{2} (A_1 \theta^2(t) + A_2 \alpha^2(t)) \geq \phi \|u\|^2, \quad (15)$$

since $\phi = \min\left(\frac{A_1}{2}, \frac{A_2}{2}\right) > 0$. This implies that $L(E, I, \theta, \alpha, t) \geq h(u)$. Consider, $\|u\|^{-1} h(u) = \|u\|^{-1} \phi \|u\|^2 = \phi \|u\|$. This gives that $\|u\|^{-1} h(u) = \phi \|u\| \rightarrow \infty$ when $\|u\| \rightarrow \infty$. Thus, condition (d) is proved. Hence, all conditions (a)-(d) shows that there exists an optimal control $u^* = (\theta^*, \alpha^*)$ that minimizes the cost functional $J(\theta(t), \alpha(t))$ over U . Therefore, the existence of optimal control is established.

□

5.3. The Hamiltonian and optimality system

We used Pontryagin's Maximum Principle [Lenhart and Workman \(2007\)](#) to drive the necessary conditions that an optimal control

must satisfy. This principle converts the objective functional (10) subject to the state system (2) into a problem of minimizing point-wise a Hamiltonian (\mathcal{H}), with respect to $\theta(t)$ and $\alpha(t)$ as:

$$\begin{aligned}
 \mathcal{H} = & B_1 E + B_2 I + \frac{1}{2} A_1 \theta^2 + \frac{1}{2} A_2 \alpha^2 \\
 & + \lambda_1 [\Pi + \eta \omega R + \nu P - \beta(\sigma_2 E + \sigma_1 I + \sigma_3 H) S - (\theta + \mu) S] \\
 & + \lambda_2 [\theta S + (1 - \eta) \omega R - (\nu + \mu) P] \\
 & + \lambda_3 [\beta(\sigma_2 E + \sigma_1 I + \sigma_3 H) S - (\delta + \mu) E] \\
 & + \lambda_4 [\tau \delta E - (\alpha + \varepsilon + \mu + \rho) I] + \lambda_5 [\alpha I - (\gamma + \mu + \xi) H] \\
 & + \lambda_6 [(1 - \tau) \delta E + \varepsilon I + \gamma H - (\omega + \mu) R],
 \end{aligned} \tag{16}$$

where $\lambda_i, i = 1, 2, 3, 4, 5, 6$, represent the adjoint variables associated with the state variables S, P, E, I, H and R to be determined suitably by applying Pontryagin's Maximal Principle [Lenhart and Workman \(2007\)](#).

Theorem 5.2. For an optimal control set θ, α that minimizes J over U , there are adjoint variables, $\lambda_1, \dots, \lambda_6$ such that:

$$\begin{aligned}
 \frac{d\lambda_1}{dt} &= [\beta(\sigma_2 E + \sigma_1 I + \sigma_3 H) + \theta + \mu] \lambda_1 - \theta \lambda_2 - \beta(\sigma_2 E + \sigma_1 I + \sigma_3 H) \lambda_3, \\
 \frac{d\lambda_2}{dt} &= -\nu \lambda_1 + (\nu + \mu) \lambda_2, \\
 \frac{d\lambda_3}{dt} &= -B_1 + \beta \sigma_2 S \lambda_1 - [\beta \sigma_2 S - (\delta + \mu)] \lambda_3 - \tau \delta \lambda_4 - (1 - \tau) \delta \lambda_6, \\
 \frac{d\lambda_4}{dt} &= -B_2 + \beta \sigma_1 S \lambda_1 - \beta \sigma_1 S \lambda_3 + (\alpha + \varepsilon + \mu + \rho) \lambda_4 - \alpha \lambda_5 - \varepsilon \lambda_6, \\
 \frac{d\lambda_5}{dt} &= \beta \sigma_3 S \lambda_1 - \beta \sigma_3 S \lambda_3 + (\gamma + \mu + \xi) \lambda_5 - \gamma \lambda_6, \\
 \frac{d\lambda_6}{dt} &= -\eta \omega \lambda_1 - (1 - \eta) \omega \lambda_2 + (\omega + \mu) \lambda_6.
 \end{aligned} \tag{17}$$

with transversality conditions

$$\lambda_i(T) = 0, i = 1, \dots, 6. \tag{18}$$

Moreover, we obtain the control set (θ^*, α^*) characterized by

$$\begin{aligned}
 \theta^*(t) &= \max \left\{ 0, \min \left(\epsilon_1, \frac{S(\lambda_1 - \lambda_2)}{A_1} \right) \right\}, \\
 \alpha^*(t) &= \max \left\{ 0, \min \left(\epsilon_2, \frac{I(\lambda_4 - \lambda_5)}{A_2} \right) \right\}.
 \end{aligned} \tag{19}$$

Proof. The form of the adjoint equations and transversality conditions are standard results from Pontryagin's Maximum Principle [Lenhart and Workman \(2007\)](#). We differentiate Hamiltonian (\mathcal{H}) (16) with respect to the state variables S, P, E, I, H and R , respectively, and then the adjoint

system can be written as

$$\begin{aligned}\frac{d\lambda_1}{dt} &= -\frac{\partial \mathcal{H}}{\partial S} = [\beta(\sigma_2 E + \sigma_1 I + \sigma_3 H) + \theta + \mu]\lambda_1 - \theta\lambda_2 - \beta(\sigma_2 E + \sigma_1 I + \sigma_3 H)\lambda_3, \\ \frac{d\lambda_2}{dt} &= -\frac{\partial \mathcal{H}}{\partial P} = -\nu\lambda_1 + (\nu + \mu)\lambda_2, \\ \frac{d\lambda_3}{dt} &= -\frac{\partial \mathcal{H}}{\partial E} = -B_1 + \beta\sigma_2 S\lambda_1 - [\beta\sigma_2 S - (\delta + \mu)]\lambda_3 - \tau\delta\lambda_4 - (1 - \tau)\delta\lambda_6, \\ \frac{d\lambda_4}{dt} &= -\frac{\partial \mathcal{H}}{\partial I} = -B_2 + \beta\sigma_1 S\lambda_1 - \beta\sigma_1 S\lambda_3 + (\alpha + \varepsilon + \mu + \rho)\lambda_4 - \alpha\lambda_5 - \varepsilon\lambda_6, \\ \frac{d\lambda_5}{dt} &= -\frac{\partial \mathcal{H}}{\partial H} = \beta\sigma_3 S\lambda_1 - \beta\sigma_3 S\lambda_3 + (\gamma + \mu + \xi)\lambda_5 - \gamma\lambda_6, \\ \frac{d\lambda_6}{dt} &= -\frac{\partial \mathcal{H}}{\partial R} = -\eta\omega\lambda_1 - (1 - \eta)\omega\lambda_2 + (\omega + \mu)\lambda_6.\end{aligned}$$

with transversality conditions

$$\lambda_i(T) = 0, i = 1, \dots, 6.$$

Similarly by following the approach of Pontryagin et al [Pontryagin \(2018\)](#), the characterization of optimal controls $\theta^*(t)$, $\alpha^*(t)$, that is, the optimality equations are obtained based on the conditions: $\frac{\partial \mathcal{H}}{\partial \theta} = 0$ and $\frac{\partial \mathcal{H}}{\partial \alpha} = 0$, which gives,

$$\theta = \frac{S(\lambda_1 - \lambda_2)}{A_1}, \quad \alpha = \frac{I(\lambda_4 - \lambda_5)}{A_2}.$$

Since θ and α are bounded in U by ϵ_1 and ϵ_2 respectively. Therefore, the optimal controls $\theta^*(t)$ and $\alpha^*(t)$ are given by

$$\begin{aligned}\theta^*(t) &= \max \left\{ 0, \min \left(\epsilon_1, \frac{S(\lambda_1 - \lambda_2)}{A_1} \right) \right\}, \\ \alpha^*(t) &= \max \left\{ 0, \min \left(\epsilon_2, \frac{I(\lambda_4 - \lambda_5)}{A_2} \right) \right\}.\end{aligned}$$

This completes the proof. □

The optimality system is formed from the state system (2) and the adjoint variable system (17) by incorporating the characterized

control set and initial and transversal condition. Then we have the following optimality system:

$$\begin{aligned}
 \frac{dS}{dt} &= \Pi + \eta\omega R + \nu P - \beta(\sigma_1 I + \sigma_2 E + \sigma_3 H)S - (\theta^* + \mu)S, \\
 \frac{dP}{dt} &= \theta^* S + (1 - \eta)\omega R - (\nu + \mu)P, \\
 \frac{dE}{dt} &= \beta(\sigma_1 I + \sigma_2 E + \sigma_3 H)S - (\delta + \mu)E, \\
 \frac{dI}{dt} &= \tau\delta E - (\alpha^* + \varepsilon + \mu + \rho)I, \\
 \frac{dH}{dt} &= \alpha^* I - (\gamma + \mu + \xi)H, \\
 \frac{dR}{dt} &= (1 - \tau)\delta E + \varepsilon I + \gamma H - (\omega + \mu)R, \\
 \frac{d\lambda_1}{dt} &= [\beta(\sigma_2 E + \sigma_1 I + \sigma_3 H) + \theta^* + \mu]\lambda_1 - \theta^* \lambda_2 - \beta(\sigma_2 E + \sigma_1 I + \sigma_3 H)\lambda_3, \\
 \frac{d\lambda_2}{dt} &= -\nu\lambda_1 + (\nu + \mu)\lambda_2, \\
 \frac{d\lambda_3}{dt} &= -B_1 + \beta\sigma_2 S\lambda_1 - [\beta\sigma_2 S - (\delta + \mu)]\lambda_3 - \tau\delta\lambda_4 - (1 - \tau)\delta\lambda_6, \\
 \frac{d\lambda_4}{dt} &= -B_2 + \beta\sigma_1 S\lambda_1 - \beta\sigma_1 S\lambda_3 + (\alpha^* + \varepsilon + \mu + \rho)\lambda_4 - \alpha^* \lambda_5 - \varepsilon\lambda_6, \\
 \frac{d\lambda_5}{dt} &= \beta\sigma_3 S\lambda_1 - \beta\sigma_3 S\lambda_3 + (\gamma + \mu + \xi)\lambda_5 - \gamma\lambda_6, \\
 \frac{d\lambda_6}{dt} &= -\eta\omega\lambda_1 - (1 - \eta)\omega\lambda_2 + (\omega + \mu)\lambda_6, \\
 \lambda_i(T) &= 0, i = 1, \dots, 6, (S(0), P(0), E(0), I(0), H(0), R(0)) = (S_0, P_0, E_0, I_0, H_0, R_0).
 \end{aligned}$$

6. Numerical simulations of optimal control problem

In this section, we perform some numerical solutions on the modified model (2) and the resulting optimality system consisting of the state equations (2) and the adjoint system (17) with the characterizations (19). We make use of the parameter values given in Table (3) for the simulation.

An iterative scheme is used to find the optimal solution of the optimality system. Since the state system (2) has initial conditions and the adjoint systems (17) have final conditions, we solve the state system using a forward fourth-order Runge–Kutta method and solve the adjoint system using a backward fourth-order Runge–Kutta method ?. The solution iterative scheme involves making a guess of the

controls and using that guess to solve the state system. The initial guess of the control together with the solution of the state systems is used to solve the adjoint systems. The controls are then updated using a convex combination of the previous controls and the values obtained using the characterizations. The updated controls are then used to repeat the solution of the state and adjoint systems. This process is repeated until the values in the current iteration are close enough to the previous iteration values [Lenhart and Workman \(2007\)](#).

We used $B_1 = B_2 = 1$, $A_1 = 40$, $A_2 = 80$ and final intervention time $T = 350$ days for simulation of COVID-19 model with optimal control. Additionally, we used $S(0) = 110079$, $P(0) = 108076$, $E(0) = 15000$, $I(0) = 13813$, $H(0) = 10050$, $R(0) = 12156$ as initial values.

6.1. Optimal control comparisons and strategies

In this subsection, we compare the results of constant and optimal control as did in ?. We first compare the cost of infection for each strategies and then compare the exposed and infected population.

The optimal control cost for each parameter is less than the constant control at all times as depicted in Figures (91) and (101). It can be observed that for protection rate θ the cost reduction is significant compared to the other parameters which is due to the high sensitivity of parameter over the system.

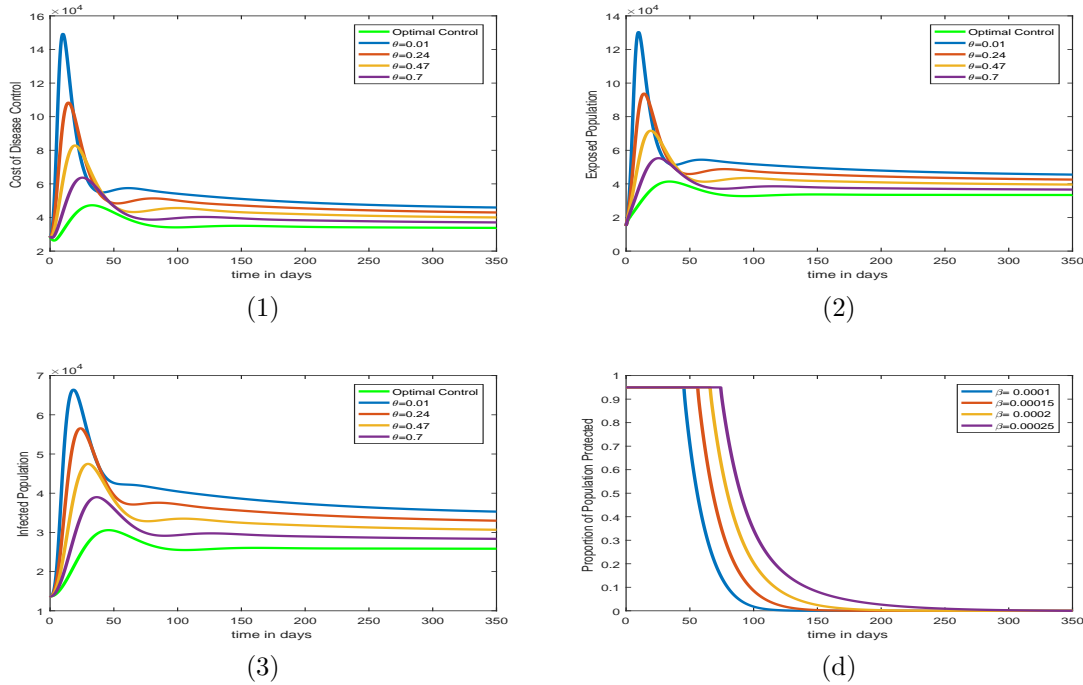


Figure 9: Optimal control for θ . (a) Cost comparison for optimal and constant controls for θ . (b) Exposed population comparison for optimal and constant controls for θ . (c) Infected population comparison for optimal and constant controls for θ . (d) Optimal strategies for θ with different β .

Now we compare the exposed population using constant and optimal controls. In Figure (92), we observe that the optimal time dependent protection strategy, θ , yields a significant drop in exposed population when compared to its constant counterparts, similarly using the optimal time dependent hospitalization strategy α we see a significant drop in the exposed population as compared to constant rates of hospitalization over time as depicted in Figure (102).

constant and optimal controls. In Figure (93), we observe that the optimal time dependent protection strategy, θ , yields a significant drop in infected population when compared to its constant counterparts, similarly using the optimal time dependent hospitalization strategy α we see a significant drop in the infected population as compared to constant rates of hospitalization over time as depicted in Figure (103).

We compare the infected population using

As contact rate β increases, so does the time for which the maximum control should be applied. In Figures (9d) and (10d), we ob-

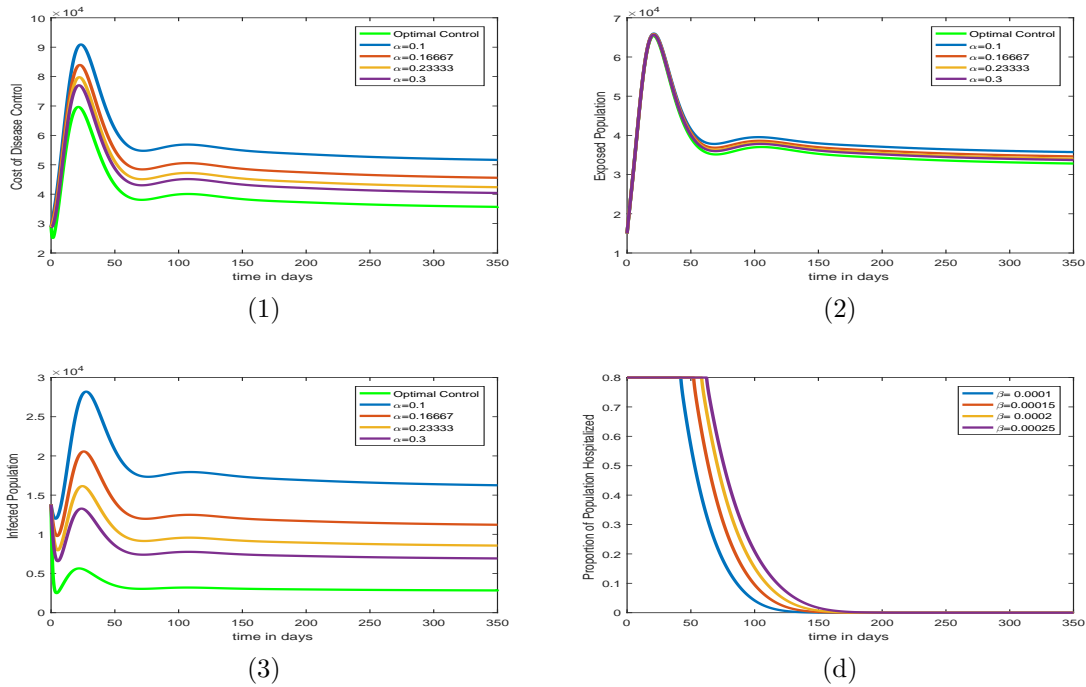


Figure 10: Optimal control for α . (a) Cost comparison for optimal and constant controls for α . (b) Exposed population comparison for optimal and constant controls for α . (c) Infected population comparison for optimal and constant controls for α . (d) Optimal strategies for α with different β .

serve that for both protection and hospitalization the maximum possible protection and hospitalization rates should be maintained to the first few days of the disease which can then be reduced over time.

Finally, from Figures (112) and (113), one can easily conclude that the combination of the two controls is significantly more effective in reducing the spread of the virus than when each control is singly applied. Hence, the best choice is to apply two controls all together to mitigate the spread of COVID-19 in the population. From Figure (111), one can observe that the combined implementation of the two control measures is the most cost-effective when compared with the single implementation of each control measure.

7. CONCLUSION

In this paper, we proposed a deterministic compartmental model to study the transmis-

sion dynamics of COVID-19. The model was an extension of the existing SEIR model by including protected and hospitalized individuals. We established the well-posedness of the modified model by proving the existence, positivity, and boundedness of the solutions.

We computed the steady states and the basic reproduction number R_0 . Based on the reproduction number R_0 , it is revealed that whenever $R_0 < 1$, the system has only disease free equilibrium e_0 which is locally as well as globally asymptotically stable. When $R_0 > 1$, the system has a unique endemic equilibrium e_1 which is locally stable and the disease free equilibrium e_0 becomes unstable. We have observed that the outbreak of the disease dies out if $R_0 < 1$ and the disease is endemic if $R_0 > 1$. Using center manifold theory, bifurcation analysis of the modified model was proven and the model exhibits forward bifurcation at $R_0 = 1$.

In addition from sensitivity analysis of R_0 , we observed that the recruitment rate Π and

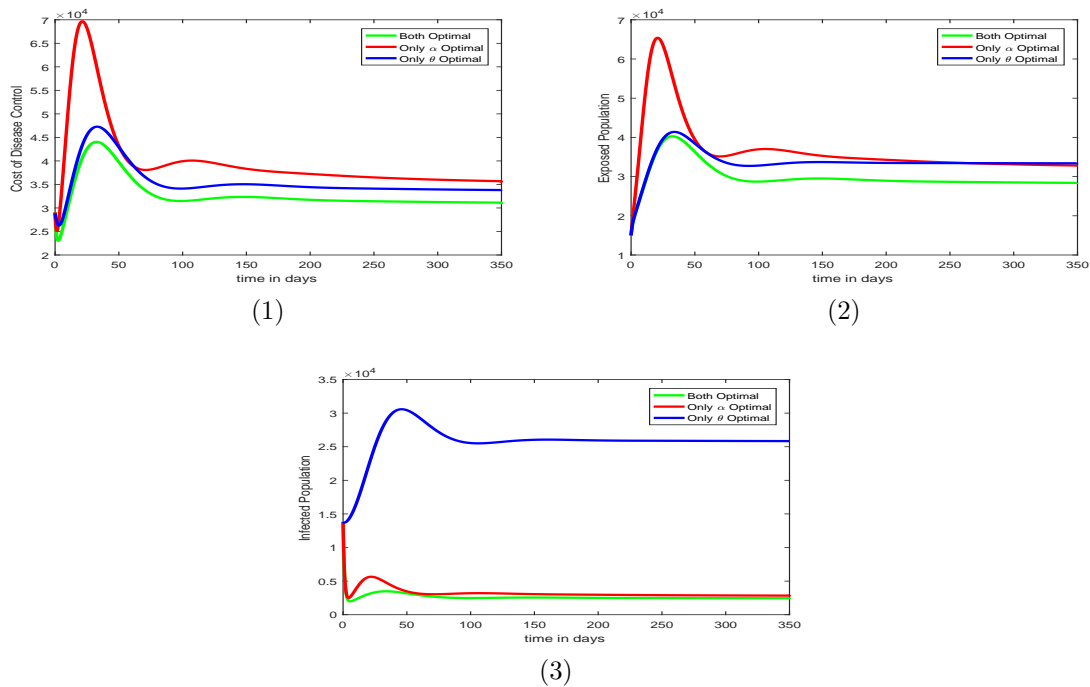


Figure 11: Optimal control for θ, α and both. (a) Cost comparison for optimal θ, α and both. (b) Exposed population comparison. (c) Infected population comparison.

contact rate β are most sensitive parameters to our model. Numerical results support the fact that decrease in the contact rate β causes the decrease in the value of R_0 and after a certain level of β , R_0 become less than one.

If the protection rate increases, then all infected classes are decrease. It is predicted that the population will be disease-free.

Furthermore, using optimal control theory we suggest protection and hospitalization strategies. Pontryagin's Maximum Principle is used to establish the existence and characterization of optimal controls. The study demonstrates that the combined application of both controls is much more effective in reducing the spread of the virus than when each control is applied individually.

Finally, our analysis indicates that an optimal control is more preferable than maintaining a high constant control.

References

- Ahmed I., Modu G. U., Yusuf A., Kummam P. and Yusuf I. (2021), 'A mathematical model of coronavirus disease (covid-19) containing asymptomatic and symptomatic classes', *Results in physics* **21**, 103776.
- Alemneh H. T. and Telahun G. T. (2020), 'Mathematical modeling and optimal control analysis of covid-19 in ethiopia', *medRxiv*.
- Allen L., Brauer F., van den Driessche P. and Wu, J. (2008), 'Mathematical epidemiology, volume 1945 of lecture notes in mathematics', *Springer, Berlin* **13**, 14.
- Bachar M., Khamsi M. A. and Bounkhel M. (2021), 'A mathematical model for the spread of covid-19 and control mechanisms in saudi arabia', *Advances in Difference Equations* **2021**(1), 1–18.
- Brauer F., Castillo-Chavez C. and Feng Z.

- (2019), *Mathematical models in epidemiology*, Vol. 32, Springer.
- Castillo-Chavez C. Blower, S. Van den Driessche P., Kirschner D. and Yakubu A.-A. (2002), *Mathematical approaches for emerging and reemerging infectious diseases: models, methods, and theory*, Vol. 126, Springer Science & Business Media.
- Castillo-Chavez C. and Song B. (2004), ‘Dynamical models of tuberculosis and their applications’, *Mathematical Biosciences & Engineering* **1**(2), 361.
- COVID-19 pandemic (2022), ‘Covid-19 pandemic in ethiopia — Wikipedia, the free encyclopedia’.
- Diekmann O., Heesterbeek J. and Roberts M. G. (2010), ‘The construction of next-generation matrices for compartmental epidemic models’, *Journal of the Royal Society Interface* **7**(47), 873–885.
- Fleming W. H. and Rishel R. W. (2012), *Deterministic and stochastic optimal control*, Vol. 1, Springer Science & Business Media.
- Gurmu E. D., Batu, G. B. and Wameko, M. S. (2020), ‘Mathematical model of novel covid-19 and its transmission dynamics’, *International Journal of Mathematical Modelling & Computations* **10**(2 (SPRING)), 141–159.
- Kifle Z. S. and Obsu, L. L. (2022), ‘Mathematical modeling for covid-19 transmission dynamics: A case study in ethiopia’, *Results in Physics* p. 105191.
- Lemecha Obsu L. and Feyissa Balcha S. (2020), ‘Optimal control strategies for the transmission risk of covid-19’, *Journal of biological dynamics* **14**(1), 590–607.
- Lenhart S. and Workman J. T. (2007), *Optimal control applied to biological models*, CRC press.
- Martcheva M. (2015), *An introduction to mathematical epidemiology*, Vol. 61, Springer.
- Pontryagin L. S. (2018), *Mathematical theory of optimal processes*, Routledge.
- Sohrabi C., Alsafi Z., O’Neill N., Khan, M., Kerwan A., Al-Jabir A., Iosifidis C. and Agha R. (2020), ‘World health organization declares global emergency: A review of the 2019 novel coronavirus (covid-19)’, *International journal of surgery* **76**, 71–76.
- Toquero C. M. (2020), ‘Challenges and opportunities for higher education amid the covid-19 pandemic: The philippine context.’, *Pedagogical Research* **5**(4).
- Valcher M. E. (2002), ‘Positive systems in the behavioral approach: main issues and recent results’, *Electronic proceedings of MTNS* **2002**.
- Yang C. and Wang J. (2020), ‘A mathematical model for the novel coronavirus epidemic in wuhan, china’, *Mathematical biosciences and engineering: MBE* **17**(3), 2708.